A Low-Complexity Orthogonal Matching Pursuit Based Channel Estimation Approach for Underwater Acoustic Baseband OFDM System

Fen Ye[1], Qinling Xie[1], Deqing Wang[1,*], Liqun Fu[1], Wen Lin[2]
[1]Key Laboratory of Underwater Acoustic Communication and Marine Information Technology (Xiamen University), Ministry of Education, Xiamen University, Xiamen 361005, China
[2]Collaborative Innovation Center of IoT Industrialization and Intelligent Production, Minjiang University, Fuzhou 350121, China
*Corresponding author: deqing@xmu.edu.cn

***Abstract*—In this paper, we propose a low-complexity Orthogonal Matching Pursuit (OMP) based channel estimation approach for underwater acoustic (UWA) baseband orthogonal frequency division multiplexing (OFDM) system, where the doubly-spread characteristic of channels is taken into account. In the proposed method, an adaptive inertia weight particle swarm optimization (AwPSO) algorithm is developed to optimize the search procedure. Subsequently, the newly proposed method, namely AwPSO-OMP, avoids calculating all Hermitian inner products of the candidates at each iteration and achieves a low computational complexity. Simulation results and experimental validation both demonstrate the effectiveness of the proposed method in UWA doubly-spread channels. Compared with the standard OMP method, the proposed method achieves the remarkable benifit in the computational complexity with the equivalent bit error rates (BERs).**

***Index Terms*—Compressed Sensing, Channel Estimation, Particle Swarm Optimization**

I. Introduction

Underwater acoustic (UWA) communications have gained increased interest over the past two decades. However, it is still quite challenging to communicate over UWA channels due to their unique characteristics. Compared with terrestrial radio channels, UWA channels exhibit excessive delay spread and severe Doppler effect. Hence, UWA channels are referred to as doubly-spread ones [1].

In order to deal with the multipath fading resulted by excessive delay spread, multicarrier transmission, e.g., orthogonal frequency division multiplexing (OFDM), has been widely adopted in UWA channels due to its low implementation complexity. For such coherent digital wireless systems, obtaining accurate estimates of the channel state information is essential. However, the aforementioned characteristics make conventional channel estimation method, e.g., least square (LS), not applicable anymore.

Fortunately, numerous studies have suggested that the channel impulse responses (CIRs) have the sparse structure. It has been shown in the literature that compressed sensing (CS) can be applied to sparse channel estimation [2]. Among existing reconstruction algorithms, orthogonal matching pursuit (OMP) is popular over UWA channels and has been verified in real field experiments [3]. The standard OMP algorithm estimates channel information utilizing over-complete dictionaries with the resolutions in delay-Doppler grid. The high resolution dictionary leads to a large number of Hermitian inner product operations. As a result, if taking the doubly-spread characteristic into account, the high computational complexity is still a burden for some special acoustic communication terminals with limited signal processing capability, e.g., the ones integrated in autonomous underwater vehicles (AUVs).

Motivated by this computational complexity problem, we focus on reducing the number of the Hermitian inner product operations to decrease the computational complexity. Considering that the operation number depends on the candidate search procedure, particle swarm optimization (PSO) algorithm can be applied to optimize the procedure. Compared with the brute force search method, the proposed one gets the best match at each iteration with less calculations. Furthermore, the PSO-assisted OMP algorithm is conducted in the baseband OFDM system. Different from the passband OFDM system, the baseband one should not solve the carrier frequency offset (CFO) problem, leading to a lower complexity in the receiver design.

The remainder of this paper is organized as follows. The system model is presented in Section II. Section III describes the proposed low computational complexity channel estimation algorithm in detail. Numerical simulations and experimental results are provided in Section IV and Section V, respectively. Finally, this paper is concluded in Section VI.

II. System Model

A. Baseband OFDM

We consider a baseband cyclic prefix OFDM (CP-OFDM) system as in [4]. Let T and T_{cp} denote the duration of an OFDM symbol and its CP, respectively. Different from the passband OFDM system defined in [3], the k-th transmitted data $s[k]$ is directly modulated at the corresponding subcarrier

through Inverse Fast Fourier Transformation (IFFT) operation. The transmitted OFDM symbol can be expressed as

$$s(t) = 2Re\left\{\sum_{k\in\mathbb{S}} s[k]e^{j2\pi f_k t}\right\} g(t), \tag{1}$$

where $\mathbb{S} = \{0, 1, \cdots, K-1\}$ denotes the index set of information data $\boldsymbol{s} = \{s[0], s[1], \cdots, s[K-1]\}^T$, and $g(t)$ is a pulse-shaping window

$$g(t) = \begin{cases} 1, & t \in [-T_{cp}, T], \\ 0, & \text{otherwise.} \end{cases} \tag{2}$$

With the sparse structure, the UWA channel can be well approximated by some dominant discrete paths [5]. Consequently, the time-varying CIRs for the UWA channels can be expressed as

$$h(t;\tau) = \sum_{\ell=1}^{N_\ell} A_\ell \delta(\tau - \tau_\ell + a_\ell t), \tag{3}$$

where N_ℓ is the number of channel paths, A_ℓ, τ_ℓ and a_ℓ are the amplitude, delay and Doppler scaling factor associated with the ℓ-th path, respectively. The amplitude and delay of the ℓ-th path are constant during the period of a CP-OFDM symbol. In [6], we resample the recieved time-domain signal after a rough Doppler estimate. The resampled signal can be expressed as

$$r(t) = \sum_{\ell=1}^{N_\ell} A_\ell s[(1+b_\ell)t - \tau_\ell] + w(t), \tag{4}$$

where b_ℓ is the residual Doppler scaling factor of the ℓ-th path, and $w(t)$ is additive ambient noise.

After Fast Fourier Transform (FFT) operation, the m-th ($m \in \mathbb{S}$) frequency-domain signal can be written as

$$z[m] = \sum_{\ell=1}^{N_\ell} A_\ell \sum_{k\in\mathbb{S}} \varrho_{m,k}^{\ell} e^{-j2\pi f_k \tau_\ell} s[k] + w[m], \tag{5}$$

where $w[m]$ is the discrete additive ambient noise and

$$\varrho_{m,k}^{\ell} = \frac{\sin(\pi \mathfrak{f}_{m,k} T)}{\pi \mathfrak{f}_{m,k} T} e^{-j\pi \mathfrak{f}_{m,k} T}, \tag{6}$$

where $\mathfrak{f}_{m,k}$ is the Doppler-induced frequency difference between the m-th and the k-th subcarriers. It can be denoted as

$$\mathfrak{f}_{m,k} = f_m - (1+b_\ell) f_k. \tag{7}$$

Stack the received data and noise as vectors $\boldsymbol{z}$ and $\boldsymbol{w}$. We can write the following input-output relationship:

$$\boldsymbol{z} = \boldsymbol{H}\boldsymbol{s} + \boldsymbol{w}, \tag{8}$$

where the channel mixing matrix $\boldsymbol{H}$ can be expressed as

$$\boldsymbol{H} = \sum_{\ell=1}^{N_\ell} A_\ell \Gamma(b_\ell)\Lambda(\tau_\ell), \tag{9}$$

where $\Gamma(b_\ell)$ and $\Lambda(\tau_\ell)$ are the matrices related with the delay and residual Doppler scaling factor of the ℓ-th path, respectively. The dimention of $\Gamma(b_\ell)$ is $R^{K\times K}$ and its off-diagonal elements represent the inter-carrier interference (ICI). The (m,k)-th element of $\Gamma(b_\ell)$ is

$$[\Gamma(b_\ell)]_{m,k} = \frac{\sin(\pi \mathfrak{f}_{m,k} T)}{\pi \mathfrak{f}_{m,k} T} e^{-j\pi \mathfrak{f}_{m,k} T}, m, k \in \mathbb{S}, \tag{10}$$

the parameter $\Lambda(\tau_\ell)$ is a $K \times K$ diagonal matrix whose (m,m)-th entry is

$$[\Lambda(\tau_\ell)]_{m,m} = e^{-j2\pi f_m \tau_\ell}, m \in \mathbb{S}. \tag{11}$$

The information data set $\boldsymbol{s}$ in Equ. (8) can be divided into a combination of a data vector $\boldsymbol{s_d}$ and a pilot vector $\boldsymbol{s}_p$, i.e., $\boldsymbol{s} = \boldsymbol{s}_d \cup \boldsymbol{s}_p$. Assume that the pilot vector $\boldsymbol{s}_p$ consists of N_P elements and is with the index set $\mathbb{P} \triangleq \{P_1, P_2, \cdots, P_{N_P}\}$. Similarly, the index set of the data vector $\boldsymbol{s}_d$ which consists of N_D elements can be denoted as $\mathbb{D} \triangleq \{D_1, D_2, \cdots, D_{N_D}\}$. The two index sets satisfy $\mathbb{P} \cup \mathbb{D} = \mathbb{S}$. In addition, the received symbols in those pilot locations can be expressed as $\boldsymbol{z}_p$. According to Equ. (8), the measurement model for channel estimation can be expressed as

$$\begin{aligned} \boldsymbol{z}_p &= \boldsymbol{H}^{\{\mathbb{P},\mathbb{P}\}}\boldsymbol{s}_p + \boldsymbol{H}^{\{\mathbb{P},\mathbb{D}\}}\boldsymbol{s}_d + \boldsymbol{w}_p \\ &= \boldsymbol{H}^{\{\mathbb{P},\mathbb{P}\}}\boldsymbol{s}_p + \boldsymbol{I_d} + \boldsymbol{w}_p \\ &= \sum_{\ell=1}^{N_\ell} A_\ell \Gamma(b_\ell)^{\{\mathbb{P},\mathbb{P}\}}\Lambda(\tau_\ell)^{\{\mathbb{P},\mathbb{P}\}}\boldsymbol{s}_p + \boldsymbol{I_d} + \boldsymbol{w}_p, \end{aligned} \tag{12}$$

where $\boldsymbol{H}^{\{\mathbb{P},\mathbb{P}\}}$ denotes the sub-matrix of $\boldsymbol{H}$ containing the rows and columns with indices in the set $\mathbb{P}$, and $\boldsymbol{H}^{\{\mathbb{P},\mathbb{D}\}}$ denotes the sub-matrix of $\boldsymbol{H}$ containing the rows with indices in the set $\mathbb{P}$ and the columns with indices in the set $\mathbb{D}$. $\boldsymbol{w}_p$ is the noise set in the pilot locations. Let $\boldsymbol{I_d} \triangleq \boldsymbol{H}^{\{\mathbb{P},\mathbb{D}\}}\boldsymbol{s}_d$ denote the ICI caused by the data subcarriers. To simplify the description in the following sections, we define $\boldsymbol{H}_p \triangleq \boldsymbol{H}^{\{\mathbb{P},\mathbb{P}\}}$, $\Lambda_p(\tau_\ell) \triangleq \Lambda(\tau_\ell)^{\{\mathbb{P},\mathbb{P}\}}$ and $\Gamma_p(b_\ell) \triangleq \Gamma(b_\ell)^{\{\mathbb{P},\mathbb{P}\}}$, and then $\boldsymbol{z}_p$ can be simplified as

$$\begin{aligned} \boldsymbol{z}_p &= \boldsymbol{H}_p\boldsymbol{s}_p + \boldsymbol{I_d} + \boldsymbol{w}_p \\ &= \sum_{\ell=1}^{N_\ell} A_\ell \Gamma_p(b_\ell)\Lambda_p(\tau_\ell)\boldsymbol{s}_p + \boldsymbol{I_d} + \boldsymbol{w}_p. \end{aligned} \tag{13}$$

For sparse UWA channels, N_ℓ is small. Consequently, $\boldsymbol{H}_p$ is parameterized by a few triplets, $\{(A_\ell, \tau_\ell, b_\ell)\}_{\ell=1}^{N_\ell}$. We only need to estimate the low-dimensional parameter sets instead of every element in $\boldsymbol{H}_p$. Furthermore, it is possible that those N_ℓ paths can be identified by CS methods.

B. Compressed Sensing-based Channel Estimation

In this paper, we adopt the OMP algorithm [7] developed in the CS context for sparse channel estimation. To solve the estimation problem with the standard OMP algorithm, we need to construct an over-complete dictionary of signal templates parameterized by a representative selection of possible parameter sets.

Following the approach in [5], an over-complete dictionary for (b_j, τ_l) can be constructed from the uniformly spaced

grids: $b_j \in \{-b_{max}, -b_{max}+\Delta b, \cdots, b_{max}\}$ and $\tau_l \in \{0, \Delta\tau, \cdots, T_{cp}\}$. In total, there are $N_b = 2b_{max}/\Delta b + 1$ tentative Doppler scales and $N_\tau = T_{cp}/\Delta\tau + 1$ tentative delays, and then $\boldsymbol{z}_p$ can be rewritten as a linear combination of all possible signal templates as

$$\begin{aligned}\boldsymbol{z}_p &= \sum_{l=1}^{N_\tau}\sum_{j=1}^{N_b}\xi_{l,j}\Gamma_p(b_j)\Lambda_p(\tau_l)\boldsymbol{s}_p + \boldsymbol{w}_p \\ &= \boldsymbol{\Psi}\boldsymbol{\xi} + \boldsymbol{w}_p. \end{aligned} \tag{14}$$

The parameter $\boldsymbol{\Psi}$ is the measurement matrix with $N_\tau N_b$ columns, and it can be denoted as the following

$$\begin{aligned}\boldsymbol{\Psi} &= [\boldsymbol{\psi}_1, \cdots, \boldsymbol{\psi}_{N_\tau N_b}] \\ &= [\Gamma_p(b_1)\Lambda_p(\tau_1)\boldsymbol{s}_p, \cdots, \Gamma_p(b_{N_b})\Lambda_p(\tau_{N_\tau})\boldsymbol{s}_p]. \end{aligned} \tag{15}$$

The parameter $\boldsymbol{\xi}$ is a $N_\tau N_b \times 1$ vector and its element $\xi_{l,j}$ is the path gains of the l-th path with the same Doppler scaling factor b_j. Most entries of $\boldsymbol{\xi}$ are zeros due to the sparseness of the channel and $\boldsymbol{\xi}$ can be denoted as

$$\boldsymbol{\xi} = [\xi_{1,1}, \xi_{1,2}, \cdots, \xi_{N_\tau,N_b}]^T. \tag{16}$$

In the standard OMP algorithm, the object is achieved through solving the following optimization problem

$$\lambda_t = \arg\max_j |\langle \boldsymbol{z}_p^{t-1}, \boldsymbol{\psi}_j\rangle|, j \notin \mathbb{I}^{t-1}, \boldsymbol{\psi}_j = \boldsymbol{\Psi}^{\{:,j\}}, \tag{17}$$

where λ_t is the index of the colunm which has the max inner products with the residual $\boldsymbol{z}_p^{t-1}$ at the t-th iteration, and $\langle\cdot,\cdot\rangle$ denotes the Hermitian inner product operation. Once the optimal column is found, the estimated τ_ℓ and b_ℓ can be obtained through searching the uniformly spaced grids for the reason that the index of each column in measurement matrix is (b_j, τ_l). After that, it solves a constrained least squares (LS) problem to get A_l of each path.

The computational complexity of the standard OMP algorithm is dominated by the number of Hermitian inner product operations. An intuitive idea to reduce the computational complexity is to decrease the number of Hermitian inner product operations. Based on this idea, we propose a PSO-assisted OMP algorithm in the following section.

III. Low Complexity Approach Design

In this section, we introduce PSO algorithm into the standard OMP channel estimation approach for the search procedure optimization.

A. The Standard PSO Algorithm

In the PSO algorithm, there are N_p particles and the i-th particle has a position x_i and a velocity v_i in the search space [8]. At the $iter$-th iteration, the position of the i-th particle can be calculated as following

$$x_i^{iter+1} = x_i^{iter} + v_i^{iter+1}. \tag{18}$$

In the proposed method, the swarm means N_p columns in the measurement matrix and the particle means one column of the swarm. Instead of searching the whole columns of the measurement matrix, PSO-assisted OMP algorithm only searches N_p columns. As a result , x_i^{iter} means the position of the i-th chosen column among N_p columns in the measurement matrix at the $iter$-th iteration. v_i^{iter+1} is the velocity of the i-th chosen column at the $(iter+1)$-th iteration and with v_i^{iter+1} changes, x_i^{iter+1} will move. The change of v_i^{iter+1} can be calculated by

$$v_i^{iter+1} = w_i^{iter}v_i^{iter} + c_1 r_1(P_{best,i} - x_i^{iter}) + c_2 r_2(G_{best} - x_i^{iter}), \tag{19}$$

where $P_{best,i}$ denotes the individual best position obtained by the i-th chosen column, G_{best} denotes the global best position among the N_p columns, r_1 and r_2 are random numbers between 0 and 1, c_1 and c_2 can be set as 2 which are the acceleration factors that pull each x_i^{iter} toward $P_{best,i}$ and G_{best} positions, and w_i^{iter} is the inertia weight at the $iter$-th iteration for the i-th chosen column. The parameter $P_{best,i}$ can be defined as the following

$$P_{best,i} = \arg\max_{x_i^\nu} f(x_i^\nu), \quad \nu \in [1, iter], \tag{20}$$

where $f(x_i^\nu) = |\langle \boldsymbol{z}_p^{\nu-1}, \boldsymbol{\psi}_{x_i^\nu}\rangle|$ is the cost function. Similarly, the global optimal position can be defined as

$$G_{best} = \arg\max_{x_i^\nu} f(x_i^\nu), \nu \in [1, iter], i \in [1, N_p]. \tag{21}$$

B. The Proposed PSO-assisted OMP Algorithm

The inertia weight w_i^{inter} in Equ. (19) is the tradeoff between the global and local search ability of particles. In order to obtain the proper value of inertia weight, we propose an adaptive inertia weight PSO algorithm named as AwPSO. As the name suggests, different from the standard PSO algorithm, the inertia weight of AwPSO will dynamically adjust according to the movement of particles.

In AwPSO, we first propose two parameters, defined as the position variance σ^{iter} and the product gap ρ_i^{iter}, respectively. The parameter σ^{iter} shows the aggregation degree of all particles at the $iter$-th iteration. Its value is defined as

$$\sigma^{iter} = \frac{1}{N_p}\sum_{i=1}^{N_p}(x_i^{iter} - G_{best})^2. \tag{22}$$

The product gap ρ_i^{iter} varies with different particles and different iteration times. The value of the i-th particle at the $iter$-th iteration can be defined as

$$\rho_i^{iter} = \frac{f(P_{best,i})}{f(G_{best})}. \tag{23}$$

The value of ρ_i^{iter} shows the cost function output ratio between the individual optimal position and the global optimal position.

The proposed two parameters σ^{iter} and ρ_i^{iter} in Equ. (22) and Equ. (23) show the practical movement process and characteristics of particles. Therefore, the adaptive inertia weight should be changed based on the two parameters and dynamically modified to keep a good balance between the

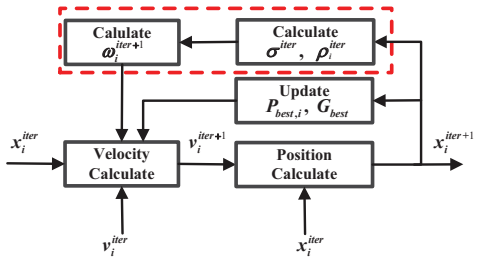

Fig. 1. Block diagram of AwPSO

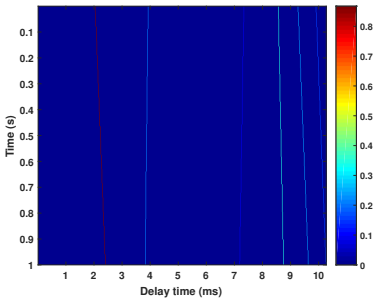

Fig. 2. A typical channel impulse response in simulations

global and the local search ability of particles. Thus, the proposed adaptive inertia weight is given by

$$w_i^{iter} = w_{ini} + w_\sigma \frac{\sigma^{iter}}{\sigma_{ini}} + w_\rho(1-\rho_i^{iter}), \tag{24}$$

where w_{ini} is the initial value of inertia weight, w_σ and w_ρ are the coefficients for σ^{iter} and ρ_i^{iter}, respectively. What's more, we normalize σ^{iter} with the initial one σ^{ini}. The value of w_{ini} is set as 0.5, while the values of w_σ and w_ρ are the same and set as 0.25. The block diagram of the AwPSO is illustrated in Fig. 1.

In AwPSO, two particles may arrive at the same position which means that the Hermitian inner product operation may be calculated repeatedly. To solve the problem, we set up a look-up table to avoid repeated computation. The binary value $b(x_i^{iter})$ is defined to show whether the position x_i^{iter} has arrived at, and it can be written as

$$b(x_i^{iter}) = \begin{cases} 1, & \text{if } f(x_i^{iter}) \text{ is calculated,} \\ 0, & otherwise. \end{cases} \tag{25}$$

Thus, the computational complexity optimization problem can be modeled as the following formulation

$$\begin{aligned} &\min \sum b(x_i^{iter}), \\ &\text{s.t.} \quad \begin{cases} iter \in [1, iter_{max}], \\ i \in [1, N_p], \\ x_i^{iter} \in D, \end{cases} \end{aligned} \tag{26}$$

where D is the problem space. When a particle arrives at a new position x_i^{iter}, it will look up the table and check the binary value $b(x_i^{iter})$. If the value of $b(x_i^{iter})$ is 1, it will get the corresponding cost function output instead of calculating the Hermitian inner product. Conversely, it will calculate the Hermitian inner product and modify $b(x_i^{iter})$ as 1 in the table.

In General, we propose the AwPSO algorithm based on the standard PSO algorithm, and apply it to the search procedure in the OMP algorithm to find the most matched column in $\mathbf{\Psi}$. In the standard OMP algorithm, the computation complexity of each path is $N_\tau \times N_b$; while the proposed method can decrease the searching times. What's more, the look-up table can further reduce the number of Hermitian inner product operations.

IV. Simulation Results

We start the simulations with a sparse channel containing 6 discrete paths. A typical CIR is shown in Fig. 2. The

TABLE I
The simulation parameters of the baseband CP-OFDM system

Parameters	Symbols	Values
Occupied frequency	$f_L \sim f_H$	$6kHz \sim 12kHz$
Sampling rate	f_s	$50kHz$
FFT size	N	4096
Subcarrier spacing	$\Delta f = 1/T$	$12Hz$
Occupied subcarriers	K	492
Starting subcarrier index	K_0	493
No. data subcarriers	N_D	369
No. pilot subcarriers	N_P	123
Symbol duration	T	$81.92ms$
CP length	T_{cp}	$25ms$
Interval of delay grid	$\Delta\tau = 1/f_s$	$0.02ms$
Interval of Doppler scale factor grid	Δb	5×10^{-5}
Delay scale dimensions	N_τ	1250
Doppler scale dimensions	N_b	21
The range of Doppler scale factor	$[b_{min}, b_{max}]$	$[-5 \times 10^{-4}, 5 \times 10^4]$

baseband CP-OFDM symbol consists of 492 occupied subcarriers, among which 123 randomly distributed subcarriers carry pilot symbols and the remaining 369 subcarriers carry data symbols. The pilot and data symbols are both modulated in a quadrature phase-shift keying (QPSK) constellation. We suppose that the common Doppler scaling factor has been estimated and the CP-OFDM symbols are resampled. That is, we only take the residual Doppler scaling factor into account. Detailed information about the simulation parameters is shown in Table. I.

For the convenience of expression, the proposed AwPSO-assisted OMP approach is denoted as AwPSO-OMP; while the standard OMP is denoted as S-OMP. We first verify the convergence performance by the success probability and the complexity benefit. The success probability means the probability that AwPSO-OMP gets the same estimate results with the S-OMP; while the complexity benefit is defined as the ratio between the reduced number of inner product operations and the total operation number in S-OMP applying brute force search procedure. As shown in Fig. 3, with the increase of the particle number, the success probability increases while the complexity benefit decreases. When the particle number is 300, the success probability reaches over 90% and the complexity benefit is 0.45. Considering the trade-off between the two metrics, we choose 300 as the particle number in the following simulations and experiments. Fig. 4 illustrates

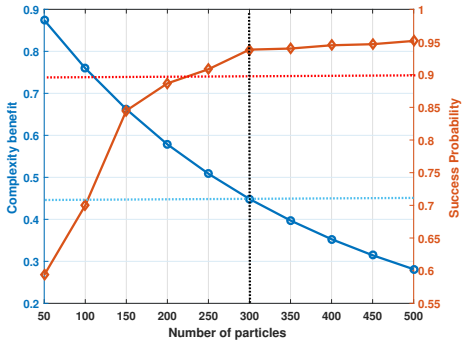

Fig. 3. Complexity benefit and Success probability of AwPSO-OMP

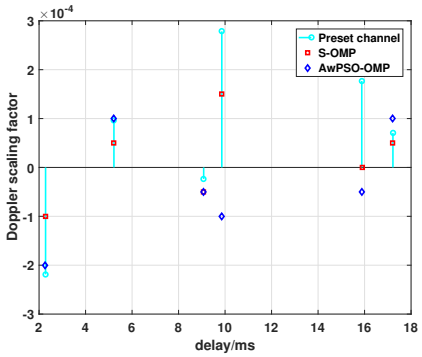

Fig. 4. Delay-Doppler scale plane

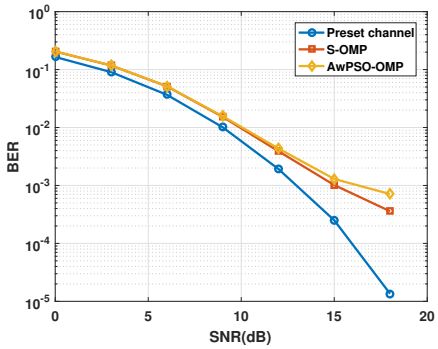

Fig. 5. Bit error rates

the distribution of the parameter sets $\{\tau_l, b_l\}_{l=1}^{N_l}$ on the delay-Doppler scale plane at a signal-to-noise ratio (SNR) of 18 dB. One can find that although the Doppler scaling factors are not exactly identical with the preset channel, AwPSO-OMP and S-OMP obtain the same delay estimation results as the preset one. Once the parameter sets are estimated, we can recover the transmitted symbols. Fig. 5 plots the bit error rate (BER) versus SNR. The result based on the preset channel state information is also shown as a lower bound. The performances of AwPSO-OMP and S-OMP are identical which demonstrates that the proposed approach can accommodate for UWA doubly-spread channels.

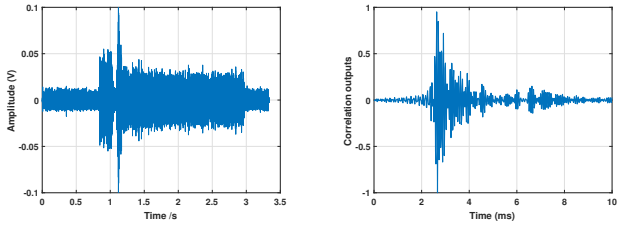

(a) The received signal in time domain (b) The corrrelation outputs

Fig. 6. The received signal in time domain and the corrrelation outputs

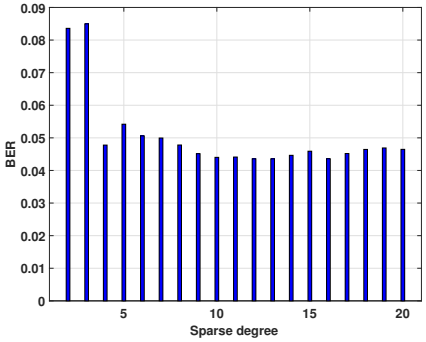

Fig. 7. BERs of S-OMP with different sparse degree

V. Experimental Validation

In order to demonstrate the performancne of the proposed approach, we further show a shallow-water acoustic communication experiment. The experiment was conducted off the coast of Xiamen, China, on December 13, 2009. The sea depth is 27m. The transmission range is 2km. Each data frame contains an preamble and 21 OFDM symbols. Each OFDM symbol consists of 410 occupied subcarriers, out of which 100 or 200 are used as pilots. Both pilot and data symbols are modulated in a QPSK constellation.

In experiments, three tones and an LFM signal are used as the preamble for rough Doppler scaling factor estimation and frame synchronization. After resampling and synchronization, the received signal is demodulated and formed the observations. A typical received data frame is plotted in Fig. 6a. One can find that the SNR is not small, but the signal is significantly influenced by the pulse noise. Another problem is to determine the number of channel paths. To solve it, we first inspect this parameter by the synchronization operation. When a local LFM signal is correlated with the received signal, the number of multipaths can be confirmed approximately. From Fig. 6b, one can see that there are about 10 multipaths with 10ms of the maximum delay spread, and then the number of grid point along the delay and Doppler scale dimensions are set as $N_\tau = 900$ and $N_b = 21$, respectively. We further calculate the BERs of S-OMP under different sparse degree shown in Fig. 7. One can see that 10 multipaths are more suitable in BER than others.

TABLE II
THE EXPERIMENTAL PERFORMANCE OF THE PROPOSED APPROACHES

Approaches	Pilot Number=100		Pilot Number=200	
	BER	Complexity benefit	BER	Complexity benefit
Doppler-Ignoring-OMP	5.85×10^{-2}	/	4.48×10^{-2}	/
S-OMP	5.86×10^{-2}	0	4.51×10^{-2}	0
AwPSO-OMP	5.87×10^{-2}	0.45	4.51×10^{-2}	0.47

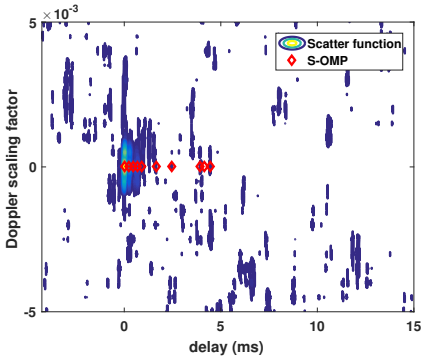

(a) S-OMP

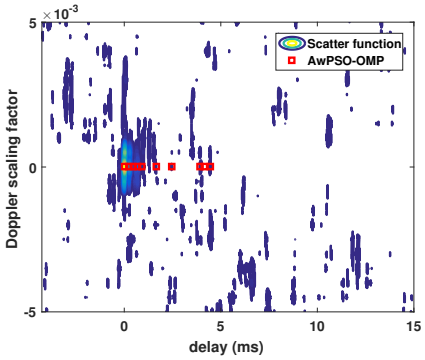

(b) AwPSO-OMP

Fig. 8. Estimation results at Xiamen experiments

Fig. 8 shows the estimation results of the proposed approach on the 2-D delay-Doppler scale plane when the pilot number is 200. From the estimation results, one can find that the residual Doppler scaling factors of multipaths in S-OMP and AwPSO-OMP are all close to zero, which matches with the results depicted by the scatter function. In order to validate the accuracy of the estimation result, we design an approach ignoring the Doppler effect for comparison, which is Doppler-Ignoring-OMP. As shown in Table. II, the BERs of S-OMP and AwPSO-OMP are equivalent to the ones of Doppler-Ignoring-OMP, which indicates that the estimations are precise when the doubly-spread characteristic is taken into account. Compared with S-OMP, AwPSO-OMP achieves the complexity benefit up to 0.45 and 0.47 with different pilot numbers. Therefore, the proposed AwPSO-OMP is more suitable to be implemented in the AUV applications with limited computational resource due to its low computational complexity.

VI. CONCLUSIONS

In this paper, we proposed a low computational complexity OMP based channel estimation approach, namely AwPSO-OMP for underwater acoustic baseband OFDM system. The approach aims to decrease the number of Hermitian inner product operations by introducing the proposed AwPSO algorithm to optimize the search procedure of finding the most matched column in the measurement matrix. The simulation and experiment results both demonstrate that the AwPSO-OMP can achieve the complexity benefit to about 0.45 while keeping the channel estimation accuracy.

ACKNOWLEDGMENTS

This work is partially supported by the National Natural Science Foundation of China (Grant No. 61771017) and the key laboratory open subject funding from Collaborative Innovation Center of IoT Industrialization and Intelligent Production, Minjiang University (Grant No. IIC1704). Qinling Xie is also supported by Undergraduate Training Program for Innovation and Entrepreneurship of Xiamen University (Grant No. 2018X0537)

REFERENCES

[1] P. Qarabaqi and M. Stojanovic, "Statistical characterization and computationally efficient modeling of a class of underwater acoustic communication channels," *IEEE Journal of Oceanic Engineering*, vol. 38, no. 4, pp. 701–717, Oct 2013.

[2] F. Qu, X. Nie, and W. Xu, "A two-stage approach for the estimation of doubly spread acoustic channels," *IEEE Journal of Oceanic Engineering*, vol. 40, no. 1, pp. 131–143, Jan 2015.

[3] B. Li, S. Zhou, M. Stojanovic, L. Freitag, and P. Willett, "Multicarrier communication over underwater acoustic channels with nonuniform doppler shifts," *IEEE Journal of Oceanic Engineering*, vol. 33, no. 2, pp. 198–209, April 2008.

[4] Y. Kim and J. Lee, "Comparison of passband and baseband transmission schemes for power-line communication ofdm systems," *IEEE Transactions on Power Delivery*, vol. 26, no. 4, pp. 2466–2475, Oct 2011.

[5] C. R. Berger, S. Zhou, J. C. Preisig, and P. Willett, "Sparse channel estimation for multicarrier underwater acoustic communication: From subspace methods to compressed sensing," *IEEE Transactions on Signal Processing*, vol. 58, no. 3, pp. 1708–1721, March 2010.

[6] J. Xu, D. Wang, X. Hu, and Y. Xie, "Doppler effect mitigation over mobile underwater acoustic ofdm system," in *the 13th ACM International Conference on Underwater Networks and Systems*, Shenzhen, China, December 2018, pp. 1–8.

[7] J. A. Tropp and A. C. Gilbert, "Signal recovery from random measurements via orthogonal matching pursuit," *IEEE Transactions on Information Theory*, vol. 53, no. 12, pp. 4655–4666, Dec 2007.

[8] C. Du, Z. Yin, Y. Zhang, J. Liu, X. Sun, and Y. Zhong, "Research on active disturbance rejection control with parameter autotune mechanism for induction motors based on adaptive particle swarm optimization algorithm with dynamic inertia weight," *IEEE Transactions on Power Electronics*, vol. 34, no. 3, pp. 2841–2855, March 2019.